Article

Longitudinal Transcriptomic, Proteomic, and Metabolomic Analyses of *Citrus sinensis* (L.) Osbeck Graft-Inoculated with "*Candidatus Liberibacter asiaticus*"

Elizabeth L. Chin, John S. Ramsey, Darya O. Mishchuk, Surya Saha, Elizabeth Foster, Juan D. Chavez, Kevin Howe, Xuefei Zhong, MaryLou Polek, Kris E. Godfrey, Lukas A. Mueller, James E. Bruce, Michelle Heck, and Carolyn M. Slupsky*

Read Online

ACCESS | Metrics & More | Article Recommendations | Supporting Information

ABSTRACT: "*Candidatus* Liberibacter asiaticus" (CLas) is the bacterium associated with the citrus disease Huanglongbing (HLB). Current CLas detection methods are unreliable during presymptomatic infection, and understanding CLas pathogenicity to help develop new detection techniques is challenging because CLas has yet to be isolated in pure culture. To understand how CLas affects citrus metabolism and whether infected plants produce systemic signals that can be used to develop improved detection techniques, leaves from Washington Navel orange (*Citrus sinensis* (L.) Osbeck) plants were graft-inoculated with CLas and longitudinally studied using transcriptomics (RNA sequencing), proteomics (liquid chromatography−tandem mass spectrometry), and metabolomics (proton nuclear magnetic resonance). Photosynthesis gene expression and protein levels were lower in infected plants compared to controls during late infection, and lower levels of photosynthesis proteins were identified as early as 8 weeks post-grafting. These changes coordinated with higher sugar concentrations, which have been shown to accumulate during HLB. Cell wall modification and degradation gene expression and proteins were higher in infected plants during late infection. Changes in gene expression and proteins related to plant defense were observed in infected plants as early as 8 weeks post-grafting. These results reveal coordinated changes in greenhouse navel leaves during CLas infection at the transcript, protein, and metabolite levels, which can inform of biomarkers of early infection.


Week 0 (Baseline) — Week 46
Navel Trees grafted with CLas (+) Budwood — Longitudinal Multi-omics Analysis Of Plant Response to CLas Infection — CLas(+) Trees Symptomatic and qPCR+
Transcriptomics (RNA-seq)
Proteomics (MS/MS)
Metabolomics (¹H NMR)
Identify changes throughout infection → understand impact of CLas on citrus metabolism

KEYWORDS: Candidatus Liberibacter asiaticus, Huanglongbing, citrus greening disease, systems biology, multiomics

■ INTRODUCTION

Huanglongbing (HLB) is a serious citrus disease associated with three species of unculturable, phloem-limited bacteria, "*Candidatus* Liberibacter asiaticus" (CLas), "*Candidatus* Liberibacter americanus" (CLam), and "*Candidatus* Liberibacter africanus" (CLaf).[1] HLB causes poor fruit quality, fruit drop, blotchy yellow mottle on leaves, and premature tree death.[2,3] The time for symptoms to appear after initial infection is variable, sometimes taking years to manifest.[1] CLas is vectored by the Asian citrus psyllid (*Diaphorina citri* Kuwayama)[4] and can also be transmitted by grafting infected material onto healthy plants.[5] CLas was first confirmed in the U.S. in Florida in 2005. HLB is now widespread in Florida and has led to a dramatic reduction in Florida's citrus acreage and yield, resulting in billions of dollars of loss to the industry.[6] Decreased fruit quality and flavors may be mitigated by blending juices, although it is becoming increasingly difficult to find unaffected fruit in Florida.[7] In 2012, one tree in Hacienda Heights, California, tested positive for CLas by quantitative polymerase chain reaction (qPCR).[8] No additional qPCR-positive trees were found until 2015,[9] but since then, more trees in California with HLB have been found. In 2018, 699 trees with HLB were found in California, representing a 160% increase in the number of diseased trees since 2017.[10] Additionally, *D. citri* has spread from southern California to northern California,[11−13] threatening all citrus trees where they exist.

Understanding pathogenesis of CLas is challenging because, until recently, the bacteria had not successfully been cultured long-term,[14] and pure cultures of CLas have yet to be maintained. Additionally, the bacteria do not have a uniform distribution and concentration throughout the tree, making the
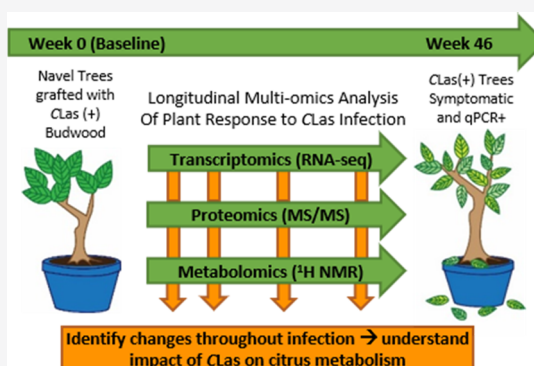
Table 1. Quantitative Polymerase Chain Reaction (qPCR) Ct Values for Control (Grafted with Clean Material) and Treatment (Grafted with Material from CLas(+) Trees) Plants from Baseline (Pregraft) up to 46 Weeks Post-Grafting (wpg)[a]

wpg	control						treatment					
	NC_1	NC_2	NC_3	NC_4	NC_5	NC_6	NH_1	NH_2	NH_3	NH_4	NH_5	NH_6
week 10	40	40	40	40	40	40	40	40	40	40	40	23.15
week 16	40	40	40	40	40	40	40	40	40	31.16	40	23.87
week 22	40	40	40	40	40	40	40	33.74	40	40	40	26.61
week 30	40	40	40	40	40	40	26.91	31.79	40	40	40	32.37
week 35	40	40	40	40	40	40	25.86	20.97	40	26.16	40	23.39
week 40	40	40	35.69 (40)	36.87 (40)	40	40	35.77	20.36	38.84	25.07	40	20.53
week 46	40	40	40	40	40	40	20.77	19.38	40	22.63	40	21.04

"Trees were designated as "positive" (infected, CLas(+)) or "negative" (uninfected, CLas(−))for CLas using the APHIS-PPQ Ct cutoff of Ct < 37 for infected trees. Values in parentheses indicate Ct values after retesting. Samples from plants with names in bold were used for analyses.

development of detection techniques and treatments for HLB challenging. However, understanding the citrus response to the pathogen offers some insight into how CLas affects citrus. Genomics, transcriptomics, proteomics, and metabolomics allow for comprehensive detection of genes, transcripts, proteins, and metabolites, respectively. These methods are complementary to each other, and the combination of multiple "omic"-based methods allows for a system-level overview of an organism.[15,16] There are several examples of systems biology approaches that have been applied to plant systems such as rice seedlings exposed to ozone,[17] irradiated maize,[18] nitrogen-deficient maize,[19] and transgenic maize lines.[20] These studies demonstrate the utility of a systems biology approach in broadening our understanding of plant systems.

Several studies have used omic technologies to investigate the effect of CLas on citrus metabolism. Metabolomic analysis of Valencia oranges revealed differences in the metabolite content of healthy, HLB-asymptomatic, and HLB-symptomatic fruits.[21,22] The concentration of several amino acids directly involved in plant defense was lower in HLB-affected fruit, suggesting that the pathogen may suppress plant defenses.[21] Similar changes in the metabolome of HLB-symptomatic Hamlin and Valencia fruits were also observed, even when fruits were harvested from different locations.[23] Transcriptomic analysis of Valencia orange leaves and fruits revealed important alterations in sucrose and starch metabolism that occur in diseased trees, leading to the disruption in the source−sink relationship.[24] Another transcriptomic study of HLB-affected Valencia fruit peel samples showed increased transcription of photosynthesis light-dependent reaction genes and higher levels of transcripts involved in protein degradation and misfolding in diseased trees, as well as induction of salicylic acid and jasmonic acid pathways.[25] A combination of proteomics and transcriptomics on CLas(+) Madam Vinous leaves found differential regulation of the stress response and transcription regulation pathways,[26] as well as changes to cell wall modification, protein degradation, and transcription regulation in CLas(+) Sanhu red tangerine roots.[27] Overall, few studies have utilized a combined multiple omics approach to study the effect of CLas on HLB development in citrus. Additionally, few are also true repeated measure (i.e., longitudinal) studies.

The objective of this work was to provide a broader and clearer understanding of the metabolic changes that occur in citrus trees infected with CLas using three omics platforms (transcriptomics, proteomics, and metabolomics) and to measure alterations over time during HLB progression. The results inform of potential biomarkers of disease and molecular

targets for treatment. Greenhouse Parent Washington Navel orange (*Citrus sinensis* (L.) Osbeck) trees were grafted with CLas-infected material (originating from Hacienda Heights, California[8]) and sampled longitudinally starting at baseline (before grafting) until severe symptom expression, which included yellow mottle on leaves, leaf drop, and overall decline in plant vigor at 46 weeks post-grafting (wpg).

■ EXPERIMENTAL SECTION

Plant Material

All plants were grown and maintained in an insect-free greenhouse at the Contained Research Facility at the University of California, Davis. The greenhouse was maintained at 27 °C (±1.5 °C) with supplemental lighting (high-pressure sodium lights; 16 h light:8 h dark). Humidity was not controlled and ranged from 30 to 50% humidity throughout the year.

Parent Washington Navel orange (or Washington navel, *C. sinensis* (L.) Osbeck) scions were grafted onto 6 month-old Carrizo rootstock. All plant materials were obtained from the University of California, Riverside Citrus Clonal Protection Program in July 2013 and were tested and certified to be free of pathogens.[28,29] For the duration of the experiment, plants were grown in 2 gallon pots in a 2:1 mixture of UC mix no. 2 and peat moss. The plants were watered as needed, and at each watering, the plants were fertilized with complete fertilizer (5-12-26) that contained the following micronutrients: magnesium (31 ppm), sulfate (SO_4 125 ppm), iron (3 ppm), manganese (0.50 ppm), zinc (0.15 ppm), copper (0.15 ppm), boron (0.50 ppm), molybdenum (0.10 ppm), and calcium (116 ppm).

In February 2014, three buds from CLas(+) or CLas(−) navel source plants were T-bud grafted onto one branch (the Navel scion) for each experimental plant. Six plants received three CLas(+) grafts (treatment), and six plants received three CLas(−) grafts (control). The three grafts were placed as close to the main stem as possible. The source plants used to obtain the buds for grafting had been assayed by qPCR for the presence of CLas using the USDA standard protocol as described by Li et al..[30] The Ct value for the CLas(+) source plant was 30.17, and the Ct value for the CLas(−) source plant was 40. The initial CLas-infected plant material was obtained from the USDA-ARS Citrus Quarantine Laboratory (Beltsville, MD).

Symptoms of HLB first appeared in one tree (NH_6) at 22 wpg, two more trees (NH_1 and NH_2) at 26 wpg, and an additional tree (NH_4) at 40 wpg. Symptoms included yellow

leaf mottle and leaf deformities. By 46 wpg, these four plants showed poor vigor and almost all leaves were symptomatic and had severe yellowing. Two trees (NH_3 and NH_5) did not exhibit HLB symptoms at any time point throughout this study.

Sampling for metabolomics, transcriptomics, and proteomics occurred between February 2014 and January 2015. Asymptomatic leaves were sampled when available (2−26 wpg); only symptomatic leaves were selected at 46 wpg. Leaves were sampled throughout the tree and were taken from multiple points around the tree canopy and included leaves that were both on the surface of the canopy as well as toward the interior. The number of leaves sampled depended on the overall size of the tree and the size of the leaves. For metabolomics, each sample consisted of 2−6 pooled leaves from a single tree and each tree was sampled at baseline and 2, 8, 10, 12, 14, 16, 18, 20, 22, 24, 26, and 46 wpg. Leaves were immediately put on dry ice and stored at −80 °C until extraction. A separate pool of 4−6 leaves from each tree was collected at 8, 18, 26, and 46 wpg and used for both transcriptomic and proteomic analyses. These leaves were immediately frozen in liquid nitrogen, put on dry ice, and then stored at −80 °C until analysis.

qPCR detection of CLas

At 10 wpg and approximately monthly thereafter, a random sampling of 6−8 leaves from each tree was pooled for qPCR analysis (Table 1). Leaves were stored at −80 °C until analysis. DNA was extracted from 200 mg (fresh weight) of leaf petioles using the Qiagen MagAttract plant DNA extraction kit (Qiagen, Valencia, CA, USA). qPCR was performed using the USDA-APHIS-PPQ protocol described by Li et al. using the HLBas and HLBr primers and HLBp probe for CLas detection and containing COX primers and probe as an internal control.[30] A tree was considered to be "positive" for CLas (CLas(+)) if the Ct value was <37 (as per the USDA-APHIS-PPQ standard) at more than one time point. Two control trees (NC_3 and NC_4) had weakly positive Ct values at 40 wpg. The exact same DNA samples were retested once and yielded negative (Ct = 40) results; we therefore believe that the initial positive results were due to sample contamination.

Transcriptomics

RNA Isolation, cDNA Library Preparation, and High-Throughput Sequencing. Four to six leaves per plant were pooled and ground in liquid nitrogen using a mortar and pestle. Total RNA was isolated from a maximum of 100 mg of frozen, ground leaf material using the Qiagen RNeasy Plant Mini Kit and treated with RNase-free DNase according to the manufacturer's instructions (Qiagen, Valencia, CA, USA). The concentration of RNA was measured using a Qubit 3.0 fluorometer (Invitrogen, Carlsbad, CA, USA), purity was measured using a NanoDrop, and quality was measured using an Agilent Bioanalyzer 2100 (Agilent Technologies, Palo Alto, CA, USA (RIN ≥ 8.0)). A total of 1 μg of RNA per sample was used for RNA sequencing (RNA-seq) of polyA-selected RNA.

Forty-eight cDNA libraries (control, n = 6; treatment, n = 6; at four time points (8, 18, 26, and 46 wpg)) for RNA-seq were generated using the Illumina TruSeq Stranded mRNA kit (Illumina, San Diego, CA, USA) with a 200 bp insert size. Libraries were size-selected to reduce the number of fragments >670 bp to improve performance on the Illumina HiSeq4000. Size selection on the final library was performed by adding 0.55× Agencourt AMPure XP beads (Beckman Coulter, Brea, CA, USA) to 15 μL of each sample library. Samples were incubated at room temperature for 5 min, beads were collected on a magnetic stand for 5 min, and the supernatant was collected. AMPure XP beads were added in to the resulting supernatant in a 1:1 ratio, the mixture was incubated at room temperature for 5 min, the beads were collected on a magnetic stand for 5 min, and then the resulting supernatant was removed. Two washes of 200 μL of 70% ethanol were performed on each sample, followed by bead resuspension in 22.5 μL of Illumina TruSeq mRNA Stranded Kit Resuspension Buffer. The mixture was incubated at room temperature for 2 min and then collected on a magnetic stand for 5 min. Twenty microliters of the resulting supernatant was collected as the final library for RNA-seq. Library concentration and quality were analyzed using a Qubit 3.0 fluorometer and Agilent Bioanalyzer, respectively. The libraries were pooled and sequenced over five lanes of an Illumina HiSeq4000 as paired-end reads (2 × 100 nucleotides) at the UC Davis Genome Center. The sequencing data has been deposited to GenBank and can be accessed at BioProject ID PRJNA417324.

RNA-Seq Processing and Data Analysis. Sequencing data was collected for all control (n = 6) and all treatment (n = 6) trees at 8, 18, 26, and 46 wpg, but only a subset of control (n = 4) and treatment (n = 4) trees were included in analyses based on qPCR results (Table 1). Raw reads were quality-checked with FastQC v.0.11.2 and then trimmed using Trimmomatic v.0.36[31] to remove low-quality bases and possible adapter contamination. The paired-end reads were then mapped to the *C. sinensis* genome (downloaded from http://phytozome.jgi.doe.gov) using TopHat2 v.2.1.1[32] with the default parameters used, except that the minimum and maximum intron lengths were set to 20 and 10,000, respectively. Raw read counts were obtained from the mapped reads using featureCounts (subread v.1.5.0)[33] at the meta-feature (exon) level. Differentially expressed genes were identified at each time point using EdgeR v.3.14.0 (q value (FDR) ≤ 0.05 and log FC ≥1.0).[34,35] The input count table from featureCounts was filtered to remove genes that did not contain at least one count per million (CPM) per sample. The total number of genes to pass this filter was 12,433, 12,652, 12,543, and 12,693 at 8, 18, 26, and 46 wpg, respectively.

GO was assigned using Blast2GO.[36] The number of differentially expressed genes that were assigned to GO terms was 193, 43, 524, and 1431 at 8, 18, 26, and 46 wpg, respectively. Lists of the differentially expressed genes were used for the input for a one-tailed Fisher's exact test in Blast2GO to identify significantly over-represented GO terms, and the resulting p values were adjusted for FDR (q ≤ 0.05). The resulting output of GO terms was reduced to the most specific terms.

Functions of the differentially expressed genes (as well as proteins and metabolites) were visualized with MapMan (v.3.6.0). Genes, proteins, and metabolites were categorized into MapMan bins using the program Mercator.[37] These MapMan bins were used to select the genes and proteins included in the bubble plots (Figure 2). MapMan does not allow different scales to be used for different marker types. Therefore, to ease visualization of the metabolite changes, metabolite markers using a different scale from the gene and protein markers were overlaid onto MapMan graphics in Adobe Illustrator.

Proteomics

Citrus Leaf Protein Extraction and Precipitation. Protein extraction was conducted at 8, 18, 26, and 46 wpg on leaves from control ($n = 4$) and treatment ($n = 4$) trees (based on qPCR results, Table 1); however, due to limitations during sample preparation, the sample size of the treatment and control groups were reduced ($n = 3$) at 8 and 46 wpg, respectively (Table S3). The same pool of ground leaves that was used for RNA-seq analysis was also used for protein extraction. Five milliliters of precipitation solvent (10% trichloroacetic acid in acetone with 2% β-mercaptoethanol) was added to 20−40 mg of ground leaf samples. Samples were vortexed, homogenized for 30 s (Kinematica Polytron), sonicated for 30 s at 15% amplitude (Branson Digital Sonifier), and stored overnight at −20 °C to allow proteins to precipitate. The resulting protein pellet was washed three times with 10 mL of ice-cold acetone. For the third acetone wash, the acetone volume added was 10× w/v of the original weighed tissue, and the protein slurry was divided into 1.5 mL aliquots, which were pelleted, dried separately, and stored at −80 °C.

Peptide Sample Preparation. Protein pellets were resuspended in 500 μL of protein reconstitution solvent (8 M urea, 100 mM triethylammonium bicarbonate (TEAB), pH 8.5 in water), vortexed, and incubated overnight at room temperature with shaking at 1400 rpm (Tomy microtube mixer MT-360). Samples were centrifuged at 16,100 × g for 10 min, and the supernatant was collected. Sample protein concentration was measured using the Quick Start Bradford protein assay (Bio-Rad, Hercules, CA). Protein samples were reduced with tris-carboxyethyl phosphine (TCEP): 5 μL of 200 mM TCEP was added to 4 μg of protein in 100 μL of TEAB and incubated at 55 °C for 1 h. Samples were briefly centrifuged at room temperature to pull down any condensation and were cooled to room temperature. Cysteine alkylation was performed by adding 5 μL of 375 mM iodoacetamide to each sample. Samples were vortexed, briefly centrifuged at room temperature to pull down condensation, and incubated for 1 h at room temperature in the dark. If necessary, 100 mM TEAB was added to samples prior to trypsin digestion to reduce urea concentration to <1 M. Sequencing grade modified trypsin (Promega, Madison, WI) was added to each sample (trypsin/protein ratio of 1:4 by weight), and samples were vortexed, briefly centrifuged at room temperature to pull down condensation, and incubated overnight at 30 °C.

C18 Column Cleanup. Dried trypsin-digested samples were resuspended in 380 μL of 0.1% formic acid in water. Samples were acidified to a pH ≤ 3 by adding 5 μL of full strength formic acid, and pH was tested via pH paper. Waters Sep-Pak C18 1 cc vacuum cartridges (cat#: WAT054955) were used with a Phenomenex vacuum manifold, with pressure kept between 4 and 5 inHg. Columns were conditioned with 3 mL of 100% acetonitrile, followed by 3 mL of 0.1% formic acid. Columns were briefly dried to remove all liquid from the column, and then samples were added and run through. Columns were then washed with 3 mL of 0.1% formic acid and briefly dried to remove all liquid from the column. Samples were eluted off the column into a collection tube by adding 500 μL of 80:20 (v/v) acetonitrile/0.1% formic acid. The column was dried to ensure that all eluent was collected. Cleaned samples were speed vacuumed (Labconco Centrivap concentrator equipped with a Savant VP100 pump) at room temperature for 1−3 h and stored at −80 °C before liquid chromatography−mass spectrometry (LC−MS) analysis.

Mass Spectrometry Analysis. Peptide samples were reconstituted with 25 μL of 95:5 acetonitrile/water (v/v) containing 0.1% formic acid and then separated by reversed-phase chromatography using a Dionex UltiMate 3000 RSLC system (Thermo Scientific, Sunnyvale, CA) equipped with a Thermo 5 mm × 300 μm trapping column packed with PepMap 100 5 cm C18 particles and a Thermo 15 cm × 75 μm Acclaim PepMap RSLC analytical column packed with C18 2 μm particles. The injection volume was 3 μL. The loading pump flow was 50 μL/min of solvent A (98:2 water/acetonitrile containing 0.1% formic acid) to load peptides on the trapping column for 6 min, followed by reversed-phase separation on the analytical column by application of a linear gradient from 95% solvent A and 5% solvent B (95:5 acetonitrile/water containing 0.1% formic acid) to 67% solvent A and 33% solvent B over 90 min with a 300 nL/min flow rate. The gradient was increased to 90% B and held for 5 min before returning to initial conditions for a 25 min re-equilibration period. Then, 2.5 kV was applied to a metal emitter tip (Thermo Scientific, Waltham, MA) in a Nanospray Flex ion source to ionize the eluted peptides, and MS was then performed using a Q-Exactive mass spectrometer (Thermo Scientific). Data-dependent analysis was performed as follows: a high-resolution MS1 scan from 300 to 2000 m/z at a resolving power of 70,000 at 200 m/z, an automatic gain control (AGC) target of 1×10^6 ions, and a maximum injection time of 120 ms. A maximum of the 12 most abundant ions in MS1 were selected for MS2 with an isolation window of 1.6 m/z and a normalized collision energy of 25, with the MS2 scans covering the range for 200−2000 m/z at a resolution of 17,500, an AGC target of 5×10^5 ions, and a maximum injection time of 60 ms. Ions included for MS2 were dynamically excluded for 30 s. Exclusion criteria for MS2 included ions with one or six or greater or undetermined charge states.

Proteomic Data Analysis. Thermo .raw files were converted into the Mascot generic format (.mgf) using MSConvert in ProteoWizard version 3.0.9393 (64-bit). A nonredundant protein database containing 166,858 proteins was created using predicted proteins from the sequenced genomes of *Citrus clementina* v.1.0, *C. sinensis* v.1.1, and CLas, as well as proteins from other citrus species from GenBank. The *C. clementina* and *C. sinensis* genomes were from Phytozome. The CLas sequences were sourced from the gxpsy, psy62, and Ishi CLas genomes. Mascot Daemon 2.3.2 (Matrix Science, Boston, MA) was used to submit .mgf files for Mascot searching against the citrus protein database. The search database included a set of 112 common contaminant proteins from yeast, bacteria, humans, and other animals. The database included the reverse sequence of all proteins as a decoy database for approximation of the false discovery rate. MS/MS search parameters included parent ion mass tolerance = 15 ppm (monoisotopic), fragment ion mass tolerance = 0.80 Da (monoisotopic), fixed modifications (cysteine/carbamidomethyl), variable modifications (asparagine; glutamine, deamidated; methionine, oxidation), and maximum one missed cleavage. Files with the .dat extension resulting from Mascot searching were loaded into Scaffold Q(+) 4.6.1 (version 4.6.1, Proteome Software, Portland, OR) and used to calculate normalized spectral counts for each protein from each sample. Scaffold protein and peptide thresholds were set at 95%, with a
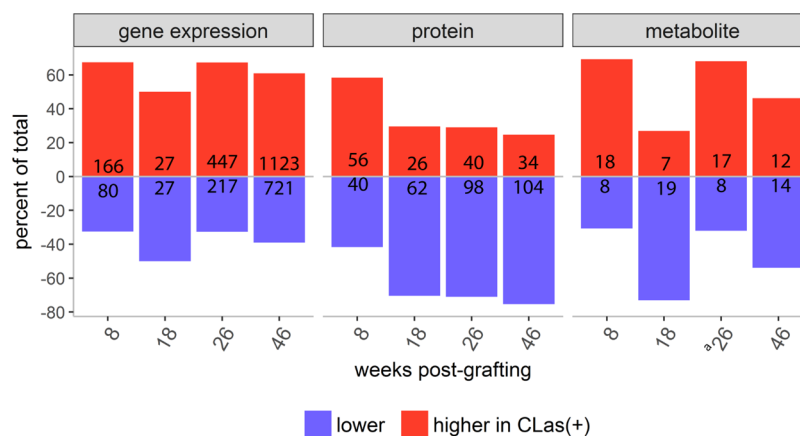
Figure 1. Percent of differentially expressed/abundant genes and proteins with a higher (red) or lower (blue) mean fold change, and percent metabolites with a higher median fold change in CLas(+) plants compared to healthy control plants at 8, 18, 26, and 46 weeks post-grafting. Numbers indicate the number of genes, proteins, or metabolites that were higher or lower. [a]Median fold change was 1.00 for one metabolite.

minimum peptide number of two per protein resulting in a protein false discovery rate (FDR) of 0.1% and a peptide FDR of 0.36%.[38,39] The cluster mode was used in Scaffold to group proteins with shared peptides and calculate weighted spectral counts. The mass spectrometry proteomic data has been deposited to the PRIDE archive (http://www.ebi.ac.uk/pride/archive)[40] via the PRIDE partner repository[41] with the dataset identifier PDX006316. During initial analysis of weighted spectral count data, proteins which had fewer than one spectral count in all biological samples were removed and not considered identified proteins. Statistical analysis of weighted spectral count data for identification of proteins differentially abundant between sample categories was performed in Scaffold with a Fisher's exact test (significance level $p < 0.05$ using the Benjamini-Hochberg multiple test correction). Gene ontology was performed on the proteomic dataset using Blast2GO as described above.

Metabolomics

Leaf samples were prepared for proton nuclear magnetic resonance (^{1}H NMR) metabolomics as described by Chin et al.[42] Approximately 15–25 leaf disks were sampled from the mesophyllic tissue, midrib and petiole from each leaf using a 6.35 mm diameter (1/4 in) hole puncher. Leaf disks were pooled and transferred to 2 mL tubes and lyophilized for 24 h (Labconco FreeZone Plus). Following this, 75 mg of dried leaf material was ground (Biospec Mini-BeadBeater 16) in a 2 mL tube with one 3.5 mm glass bead for two 1 min intervals with a 30 s break in between intervals. Phosphate buffer (10 mM, pH 6.8) heated to 90 °C was added to the ground leaf material in a 1:20 (w/v) ratio based on the dry weight of the leaf sample used and mixed for 15 min at 90 °C at 1000 rpm (Eppendorf ThermoMixer C). Samples were then centrifuged at 4 °C for 15 min at 14,000 × g. The resulting supernatant (750 μL) was collected and centrifuged at 4 °C for 15 min at 14,000 × g. Sixty-five microliters of internal standard containing 5 mM 3-(trimethylsilyl)-1-propanesulfonic acid-d_6 (DSS-d_6) was added to 585 μL of the resulting supernatant, and 600 μL of the subsequent mixture was transferred to 5 mm NMR tubes and stored at 4 °C until NMR data acquisition (within 24 h of sample preparation).

^{1}H NMR was performed as described by Chin et al.[42] using a Bruker Advance 600 MHz NMR spectrometer equipped with a SampleJet. The Bruker "noesypr1d" (RD-90°-t-90°-t$_m$-ACQ)

experiment was used. The acquisition parameters were as follows: 12 ppm sweep width, 2.5 s acquisition time with 2.5 s relaxation delay, and 100 ms mixing time with water saturation applied during the relaxation delay and mixing time; spectra were zero-filled with 128,000 data points, the number of scans was 32, and an exponential apodization function corresponding to a line broadening of 0.5 Hz was applied. Metabolites were identified and quantified using Chenomx NMR suite v7.6 (Chenomx Inc., Edmonton, Alberta, Canada) and corrected for dilution. Although ^{1}H NMR data was collected for all treatment ($n = 6$) and all control ($n = 6$) trees, only the subset of treatment trees that tested qPCR(+) (Ct < 37) at multiple time points ($n = 4$) and the subset of control trees that consistently tested qPCR(−) ($n = 4$, Table 1) were included in statistical analyses, with the exception of 26 wpg, where for treatment $n = 3$, as one tree's samples were unusable due to improper storage.

Partial least-squares-discriminant analysis (PLS-DA) was performed using SIMCA-P v13.0.3 with unit variance scaling on log$_{10}$-transformed data. The Mahalanobis distance was used to quantify the distance between group centroids in the PLS-DA plots, and a two sample Hotelling's T^2 test was used to determine if the cluster separation was statistically significant with $\alpha = 0.05$ in R v3.4.1.[43] The metabolomics data have been deposited to citrusgreening.org and can be accessed at https://citrusgreening.org/metabolomics_host/index.

■ RESULTS

qPCR

qPCR was performed approximately every month starting at 10 wpg (Table 1). A tree was considered qPCR-positive for CLas using the APHIS-PPQ cutoff of Ct < 37. By the end of the experiment (46 wpg), four of the six treatment trees that were grafted with infected budwood had tested CLas(+) by qPCR at multiple time points (Table 1). One treatment tree (NH_3) had a non-40 Ct value above the APHIS cutoff at 38 wpg (Ct = 38.84) and no obvious visual symptoms of HLB and was not included in statistical analyses. Among control trees, four of the six control trees consistently tested CLas(−) throughout the experiment (Table 1). Two control trees (NC_3 and NC_4) had weakly positive Ct values at 40 wpg; however, retesting the same DNA samples yielded negative (Ct = 40) results. Trees that repeatedly tested positive and negative for CLas were used

Table 2. Top 10 GO Terms for Each Time Point with the Lowest FDR Values (FDR < 0.05)[a]

GO ID	GO name	GO category	8 wpg		18 wpg		26 wpg		46 wpg	
			gene	protein	gene	protein	gene	protein	gene	protein
GO:0004332	fructose-bisphosphate aldolase activity	M				down				down
GO:0004568	chitinase activity	M				up	up	up		up
GO:0004857	enzyme inhibitor activity	M					up		up	
GO:0004866	endopeptidase inhibitor activity	M				down				
GO:0005267	potassium channel activity	M					down			
GO:0005576	extracellular region	C					down			
GO:0005618	cell wall	C					up			
GO:0006032	chitin catabolic process	B				up	up	up		up
GO:0006096	glycolytic process	B				down				down
GO:0006355	regulation of transcription, DNA-templated	B					down			
GO:0009506	plasmodesma	C					up		up	
GO:0009522	photosystem I	C		down		up			down	
GO:0009535	chloroplast thylakoid membrane	C						down	down	down
GO:0009538	photosystem I reaction center	C				down				down
GO:0009654	photosystem II oxygen evolving complex	C						down	down	down
GO:0009664	plant-type cell wall organization	B				up			up	
GO:0009765	photosynthesis, light harvesting	B							down	
GO:0009768	photosynthesis, light harvesting in photosystem I	B		down				down		down
GO:0009941	chloroplast envelope	C		down				down		down
GO:0010043	response to zinc ion	B				down				
GO:0010287	plastoglobule	C		down				down		down
GO:0010951	negative regulation of endopeptidase activity	B				down		up		up
GO:0015979	photosynthesis	B				down				
GO:0016168	chlorophyll binding	M		down				down	down	down
GO:0016998	cell wall macromolecule catabolic process	B				up		up		up
GO:0018298	protein-chromophore linkage	B		down				down	down	down
GO:0019898	extrinsic component of membrane	C						down	down	down
GO:0031409	pigment binding	M		down				down		down
GO:0031977	thylakoid lumen	C						down		down
GO:0042744	hydrogen peroxide catabolic process	B								down
GO:0043086	negative regulation of catalytic activity	B					up		up	
GO:0045490	pectin catabolic process	B					up		up	
GO:0046872	metal ion binding	M						down	down	
GO:0055114	oxidation—reduction process	B						down	down	down
GO:0071805	potassium ion transmembrane transport	B					down			

[a]Determined by a one-tailed Fisher's exact test (FDR < 0.05) performed on genes and proteins with higher ("up") or lower ("down") expression/abundance in infected plants versus controls. GO category: B = biological process, C = cellular component, and M = molecular function.

as selection criteria for infected treatment and uninfected control trees, respectively. Therefore, four treatment and four control trees were used in all analyses with the exception of 26 wpg for metabolomics (treatment, $n = 3$) and 8 wpg (treatment, $n = 3$) and 46 wpg (control, $n = 3$) for proteomics due to sampling limitations.

Transcriptomics

RNA extracted from leaf samples obtained at 8, 18, 26, and 46 wpg was used for construction of cDNA libraries and sequenced on an Illumina HiSeq4000 (PE100). The number of differentially expressed genes at 8, 18, 26, and 46 wpg were 246, 54, 664, and 1844, respectively ($|\log_2 FC| \geq 1$ and $q \leq 0.05$; Table S1). At 8 and 26 wpg, the number of differentially expressed genes with higher expression levels in CLas(+) plants compared to controls was almost two times greater than the number of genes with lower expression levels (Figure 1). At 18 wpg, the number of genes with higher expression levels in CLas(+) plants was equal to the number with lower levels (Figure 1).

At 8 and 18 wpg, no gene ontology (GO) terms were significantly over-represented among the differentially expressed genes (Table 2 and Table S2). Nonetheless, at 8 wpg, several genes involved in phenylpropanoid metabolism were differentially expressed; specifically, expressions of 4-coumarate-CoA ligase (4CL), cinnamoyl-CoA reductase (CCR), and cinnamyl alcohol dehydrogenase (CAD) were higher in infected plants (Figure S1). Relatively few genes were differentially expressed at 18 wpg compared to the other time points; these included three genes encoding for expansins (two with higher expression levels in CLas(+) and one lower in CLas(+)), as well as one Kunitz family trypsin and protease inhibitor gene (lower levels in CLas(+)) (Table S1). (These genes are annotated as "Kunitz family trypsin and protease inhibitor" (Phytozome) and "miraculin" or "miraculin-like" (Blast2GO) (Tables S1−S3). Miraculin and miraculin-like proteins have trypsin inhibitor activity and sequence similarity with soybean Kunitz family trypsin inhibitors.[44,45] For clarity, only Kunitz family trypsin and protease inhibitor will be further used.)

At 26 wpg, cell wall modification genes (represented by pectinesterases, pectate lyases, and glucan endo-1,3-β-glucosidases) and chitinase genes had higher expression in CLas(+) plants (Table 2). Expression of pectin methylesterase inhibitor (PMEI) family genes (GO: enzyme inhibitor activity) was higher in infected plants (Table 2). Additionally, although related GO terms were not over-represented, genes involved in phenylpropanoid metabolism, including 4CL, caffeoyl-CoA O-methyltransferase (CCoAMT), and caffeic acid O-methyltransferase (COMT), had higher expression levels in infected plants. CCR and CAD, however, had lower expression (Figure S1).

At 46 wpg, photosynthesis gene expression was lower in CLas(+) plants than controls (Figure 2). Genes directly associated with photosynthesis (photosystem I- and photosystem II-encoding genes (PSI and PSII, respectively), and RuBisCO) and those associated with chlorophyll/chloroplasts and thylakoid had lower expression levels in infected plants (Table 2 and Figure S2). Gene expression related to cell wall modifications was higher in CLas(+) plants (Table 2 and Figure 2), which included genes encoding xyloglucan endotransglycosylases, pectate lyase, pectinesterases, and glycosyl hydrolase/endoglucanases. PMEI gene expression was also higher in CLas(+) plants relative to controls. Several genes in the phenylpropanoid pathway were differentially expressed, although related GO terms were not over-represented at 46 wpg (Figure S1).

Proteomics

Tandem mass spectrometry (MS/MS)-based proteomics was conducted at 8, 18, 26, and 46 wpg. A total of 382 proteins were identified from all samples at all time points (Table S3), of which 248 were found to be differentially abundant between CLas(−) and CLas(+) grafted trees at one or more of the four time points analyzed (Table S4). At 8 wpg, the number of proteins with higher abundance in CLas(+) plants (56) was greater than the number with higher abundance in control plants (40) (Figure 1). At 18, 26, and 46 wpg, however, more proteins had higher abundance in control plants compared to infected plants (Figure 1). At 46 wpg, 104 proteins were found to be more abundant in CLas(−) compared to CLas(+) plants, while only 34 proteins were found to be more abundant in CLas(+) compared to CLas(−) plants.

At 8 wpg, photosynthesis-related proteins had lower abundance in CLas(+) plants (Figure 2). Most PSII and ATP synthase proteins had lower abundance in CLas(+) plants compared to controls (Figure S2 and Table S2). Proteins involved in the plant stress response were overall more abundant in infected plants at 8 wpg (Figure 2). Six Kunitz family trypsin and protease inhibitors had higher levels in infected plants, and one was slightly lower, although no trypsin inhibitor genes were differentially expressed at 8 wpg (Figure S3 ("PR-proteins")).

At 18 wpg, chitinase proteins were more abundant in infected plants, and proteins involved in protein degradation were less abundant (Table 2). Photosynthesis proteins were overall less abundant in infected plants compared to controls (Figure 2), including most PSI reaction center proteins (Table 2 and Figure S2). Five Kunitz family trypsin inhibitors had higher levels, and one had lower levels at 18 wpg (Figure S3 (PR-proteins)).

At 26 wpg, chitinase proteins were more abundant in infected plants (Table 2). Negative regulation of endopepti-
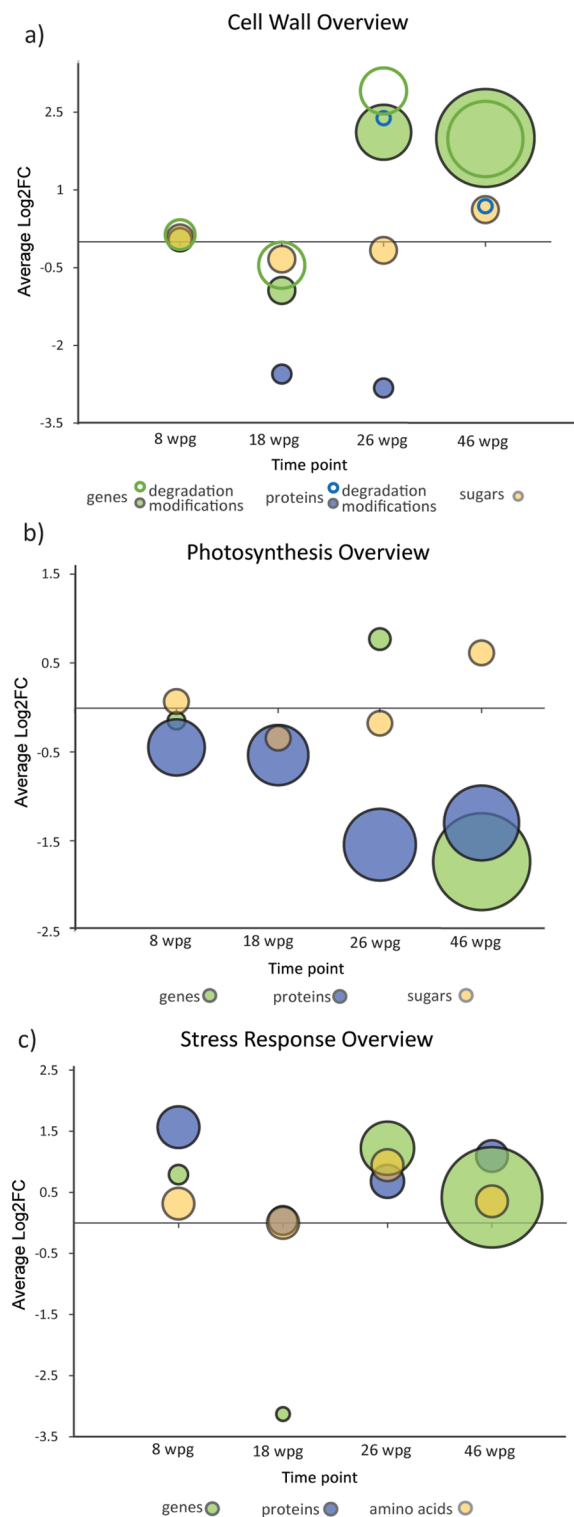

Figure 2. Overview of the average log$_2$ FC of genes (green), proteins (blue), and metabolites (yellow) involved in (a) cell wall metabolism, (b) photosynthesis, and (c) stress response at 8, 18, 26, and 46 wpg. The area of each marker is scaled to the number of genes, proteins, or metabolites.

dase activity was observed, corresponding to five Kunitz family trypsin inhibitor proteins (all higher in infected plants), two serine protease inhibitor proteins (both higher), and a cysteine protease inhibitor protein (lower) (Table S4). Although seven Kunitz family trypsin inhibitor proteins had higher levels in

infected plants compared to controls at 26 wpg, no related genes were differentially expressed (Figure S3 ("PR-proteins") and Tables S1 and S4)). Photosynthesis proteins, including PSI proteins and a subunit for RuBisCO, were less abundant in infected plants at 26 wpg (Figure S2 and Table 2).

At 46 wpg, photosynthesis proteins were also less abundant in infected compared to healthy plants (Figure 2), including proteins involved with photosystem II oxygen evolving complex, protein-chromophore linkage, chlorophyll binding, and thylakoid membrane (Table 2 and Figure S2). Many of the same GO terms were also downregulated in the transcriptome data at 46 wpg (Table S2). Indeed, several RuBisCo-related and Calvin cycle-related proteins were less abundant in CLas(+) plants at 46 wpg (Figure S2). Similar to 18 and 26 wpg proteins, chitinase levels were also higher in infected plants.

Metabolomics

^{1}H NMR metabolomics was conducted at baseline and 2, 8, 10, 12, 14, 16, 18, 20, 22, 24, 26, and 46 wpg. Twenty-six metabolites were identified and quantified for each sample; these included carbohydrates, amino acids, and organic acids, as well as several other small molecules, including one unknown molecule ("unknown-1"), which was identified by singlet peaks at 2.9 and 4.1 ppm.

Metabolite concentrations were highly variable over time and between plants (Table S5), and thus, differences in metabolite concentrations between control and infected plants at specific time points did not reach statistical significance (using repeated measures ANCOVA using baseline as the covariate). The metabolome is highly dynamic and complex, and a single metabolite may participate in several metabolic pathways or interact with multiple enzymes.[46,47] Even small stimuli, such as slight changes in light or temperature, can change plant metabolism and be reflected in the metabolome.[48] One key constraint in the experiment was sample size. Only four plants per group were analyzed, which may not have been sufficient to establish statistical significance for many of the metabolites. Nonetheless, we observed trends in the metabolite changes between control and CLas(+) plants during infection.

Partial least-squares-discriminant analysis (PLS-DA) was used to determine differences in the leaf metabolome between infected and control plants; samples from all time points were included in the model to determine differences that were independent of time (Figure 3, $R^2X = 0.323$, $R^2Y = 0.452$). Permutation testing (100 permutations) indicated a valid model. The Mahalanobis distance between the centroids of the two groups (control and infected) along components 1 and 2 was 1.92, and a two sample Hotelling's T^2 test indicated significant separation between the centroids of the two groups (calculated F value = 28.29; critical F value = 3.09; α = 0.05). The resulting PLS-DA loading plot (Figure 3) and variable importance on the projection (VIP) scores (≥ 1) were used to identify metabolites that were higher or lower in infected plants compared with control throughout infection. Specifically, uridine, cytidine, asparagine, aspartate, choline, and synephrine were generally lower in the infected plants compared with control plants from 14 to 22 wpg (Figure 4). Proline, proline betaine, limonin glucoside, and trigonelline were higher in the infected plants compared to controls at most time points (Figure 4).
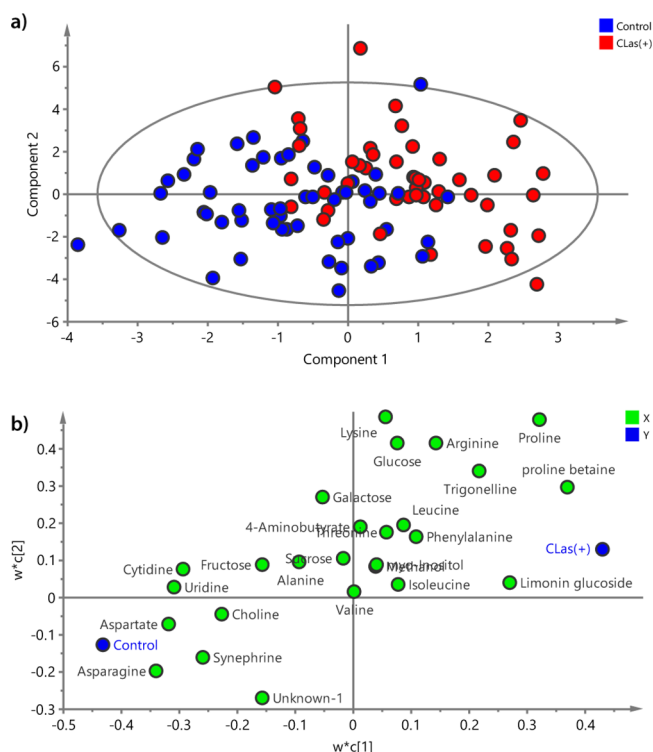

Figure 3. (a) Partial least-squares-discriminant analysis score plot of control (blue) and CLas(+) (red) Navel leaf samples at baseline and 2, 8, 10, 12, 14, 16, 18, 20, 22, 24, 26, and 46 wpg and (b) corresponding loading plot. At baseline, both control and treatment plants are considered CLas(−) because it was pregraft. $R^2X = 0.323$; $R^2Y = 0.452$; $Q^2 = 0.254$.

There were several metabolites that did not contribute to the observed separation in the PLS-DA plot but changed over the course of the infection (Figures 3 and 4). Specifically, fructose, glucose, and sucrose were mostly higher in infected plants at 8, 10, and 12 wpg but lower in concentration at 18, 22, and 24 wpg (Figure 4). Notably, sucrose and glucose concentrations were higher in all infected plants at 46 wpg compared to controls, when photosynthesis transcripts and proteins were less abundant in infected plants (Table 2 and Figure 2). Additionally, the median phenylalanine concentration was higher in infected plants relative to control at 8 and 12 wpg, as well as at 26 wpg, when multiple genes involved in the phenylpropanoid pathway were differentially expressed (Figure S1).

■ DISCUSSION

This study utilized a systems biology approach to understand CLas-induced perturbations in a citrus host over time. Greenhouse Navel trees were graft-inoculated with the Hacienda Heights, California, isolate of CLas, and leaves were analyzed to determine differences in the transcriptome, proteome, and metabolome between infected and uninfected plants over the course of 46 weeks.

CLas Infection Alters Photosynthesis

A substantial decrease of photosynthesis-related gene expression and protein abundance was observed in CLas(+) plants relative to controls at 26 and 46 wpg, and lower protein abundance was also observed at all time points in infected plants (Figure 2). Others have also found downregulation of photosynthesis genes and proteins during CLas infec-

Metabolite		0	2	8	10	12	14	16	18	20	22	24	26	46
		weeks post-grafting												
Sugars	Fructose	0.86	0.79	1.26	1.52	1.00	0.89	1.46	0.99	0.99	0.71	0.41	0.39	1.02
	Glucose	0.68	1.56	1.14	1.73	1.18	0.95	1.21	0.64	1.23	0.76	0.72	2.09	3.47
	Sucrose	1.23	0.93	0.87	1.27	1.70	1.22	0.92	0.75	1.15	0.89	0.74	0.61	1.35
	Galactose	1.07	1.02	0.98	1.41	1.15	1.15	0.80	0.84	0.84	0.98	0.98	1.28	1.17
Amino Acids	Alanine	0.92	0.60	1.05	1.32	1.39	0.95	0.91	0.77	1.01	0.99	0.76	1.03	1.22
	Valine	1.10	1.03	1.33	0.91	1.43	0.47	0.76	1.98	0.63	1.39	0.92	2.31	0.88
	Leucine	1.23	1.03	1.73	0.92	1.31	0.78	1.17	0.96	0.74	1.27	0.85	2.71	1.20
	Asparagine	0.87	1.15	0.72	0.72	0.58	0.56	0.48	0.95	0.40	0.67	0.21	1.90	0.48
	Aspartate	0.88	0.93	0.82	0.58	0.45	0.76	0.60	0.45	0.52	0.49	0.42	1.15	2.28
	Threonine	1.11	1.09	1.60	1.14	1.64	0.64	0.87	1.15	0.71	1.02	0.75	1.84	0.95
	Isoleucine	1.08	0.87	1.61	1.23	1.10	0.43	0.94	1.37	0.67	1.31	1.10	3.21	0.65
	Lysine	0.88	0.97	1.59	1.35	1.16	0.73	0.56	1.47	0.49	0.86	0.68	1.36	3.31
	Phenylalanine	1.10	0.91	1.24	1.05	1.71	0.86	1.08	1.06	0.84	0.98	0.97	2.16	0.92
	Arginine	0.53	1.36	1.09	0.87	1.59	1.34	1.37	0.80	0.90	1.24	1.01	3.23	4.21
	Proline	1.22	1.15	1.41	1.32	1.33	1.07	1.52	0.83	1.12	1.31	1.27	1.70	1.35
Others	Proline Betaine	1.12	1.11	1.10	1.31	1.35	0.90	1.00	0.94	1.20	1.59	0.86	1.28	0.87
	4-Aminobutyrate (GABA)	1.03	0.60	0.94	0.97	2.91	1.38	0.90	0.96	1.09	1.04	0.90	1.37	0.54
	Uridine	1.16	0.91	1.21	1.16	0.93	0.81	0.56	0.72	0.88	0.78	0.61	0.76	0.96
	Cytidine	1.08	1.08	1.16	1.14	1.01	0.77	0.55	0.76	0.78	0.79	0.40	0.93	0.83
	Choline	1.34	0.95	1.02	1.11	1.30	0.96	0.80	0.89	0.89	1.03	0.66	0.65	0.85
	Synephrine	0.91	1.08	0.90	1.16	0.71	0.67	0.45	0.86	0.92	0.81	0.41	0.48	0.85
	Methanol	1.36	1.09	1.10	1.19	1.33	0.95	0.77	0.81	1.11	1.03	0.75	1.00	0.96
	Unknown-1	1.18	0.67	1.49	1.09	1.02	0.68	0.80	0.64	1.23	1.27	0.91	0.92	0.55
	myo-Inositol	1.26	1.02	1.08	1.17	0.96	0.85	0.64	0.87	1.42	0.90	0.85	0.97	1.17
	Trigonelline	0.88	1.20	0.93	2.19	1.57	1.44	0.89	1.24	1.05	1.17	0.72	1.08	1.43
	Limonin glucoside	1.02	1.17	0.82	1.16	1.25	1.05	1.64	1.53	1.90	1.89	0.81	2.31	0.55

Figure 4. Fold change of median metabolite concentrations (infected relative to control) at each time point (wpg). Red indicates a higher median concentration, and blue indicates a lower median concentration in CLas(+) plants relative to controls. Bold borders indicate time points at which transcriptomic and proteomic analyses were also conducted.

tion,[24,49−52] although upregulation of light reaction genes in symptomatic fruit has also been reported.[24,25] Negative regulation of photosynthesis during infection or in the presence of other stressors has been reported, which is thought to help channel resources for defense.[53,54]

These changes in photosynthesis gene expression and protein abundance corresponded to changes in sugar concentrations (Figure 2). Given reports of carbohydrate and starch accumulation within the leaves of HLB-affected citrus,[55−58] it is possible that this accumulation of sugars further inhibits photosynthesis.[59] We observed the largest effect of CLas on photosynthesis at the gene, protein, and metabolite levels at 46 wpg.

CLas Infection Induces Cell Wall Changes

Substantial changes to cell wall-related gene expression and protein abundance were observed at 26 and 46 wpg (Table 2, Figure 2). Cell wall modifications improve the physical barrier between the plant and pathogen,[60,61] which may be especially important for HLB given the phloem-limited nature of CLas. A meta-analysis of microarray data found upregulation of cell wall probe sets in CLas resistant citrus varieties at 17 wpg but downregulation in susceptible varieties during infection.[62] Cellulose synthase (26 and 46 wpg) and callose synthase (46 wpg) gene expressions were higher in infected plants compared to controls (Table S1). Regulation of cellulose synthase during HLB is mixed and appears to depend on the variety and organ.[25,52,63,64]

Additionally, changes in gene expression of lignin synthesis via the phenylpropanoid pathway was observed (Figure S1). Like cellulose, lignin strengthens the cell wall and increased synthesis can occur in response to pathogens.[65] The hydroxycinnamyl alcohols coniferyl, sinapyl, and p-coumaryl alcohols, are the main monolignol building blocks of lignin and

are synthesized from phenylalanine.[66] Exogenous application of phenylalanine was shown to increase the production of the p-coumaryl alcohol and coniferyl alcohol, as well as the transcripts for PAL, 4CL, CCoAMT, and CCR, which are involved in lignin biosynthesis, in pine.[67]

At 8 wpg, the median phenylalanine concentration was higher in CLas(+) plants compared to controls, and expression of genes involved in hydroxycinnamyl alcohol synthesis (4CL, CCR, CAD) was higher in infected plants (Figure S1). At 26 wpg, phenylalanine concentration was also higher in CLas(+) plants and the expression of 4CL was higher in CLas(+) plants while CAD expression was lower. CAD deficiency has been shown to lead to the incorporation of the hyroxycinnamalde-hyde monomers into lignin.[68−70] Indeed, at 46 wpg, phenyl-alanine concentration was similar between control and infected plants (Figure 4), and CAD expression was lower. Laccase, which polymerizes monolignols, had higher expression in CLas(+) plants at 46 wpg (Figure S1). Taken together, the gene expression profile suggests a shift toward hydroxycinna-maldehyde synthesis and incorporation into lignin at 26 and 46 wpg.

Additionally, gene expression for expansins (GO: plant-type cell wall organization) was higher in CLas(+) plants relative to controls at 26 and 46 wpg (Table 2). Similar findings have been observed with Mexican lime trees infected with the phloem-limited pathogen that causes witches' broom disease; expansin proteins were more abundant, and gene expression was upregulated in infected plants.[71,72] Expansins promote cell growth by loosening the cell walls, and enhanced expansin expression could therefore make the cell wall vulnerable and improve CLas mobility.[73]

CLas Infection Increases Cell Wall Degradation

The expression of genes and proteins involved in cell wall degradation changed throughout infection (Figure 2). Expression of several β-glucanase and glucan endo-1,3-β-glucosidase genes and one β-glucanase protein was higher in CLas(+) plants at 26 and 46 wpg (Figure S3 and Table S2). β-glucanase and glucan endo-1,3-β-glucosidases cleave the β-1,3-glucosidic linkages in callose, releasing glucose. Our observation of substantial changes in β-1,3-glucanase expression during late stages of CLas infection is consistent with previous studies.[26,52,64,74] Higher levels of glucan endo-1,3-β-glucosidase gene expression levels may result from an effort by the plant to reduce cell wall occlusion. Conversely, this may represent an opportunity for the pathogen to further spread throughout the plant. For example, tobacco plants expressing antisense β-1,3-glucanases are less susceptible to viruses.[75] Therefore, increased callose degradation by inducing cell wall degradation may weaken barriers to CLas spread and enable systemic infection.

Cellulase gene expression was higher in CLas(+) plants at 46 wpg (Table S2). This is consistent with previous studies showing upregulation of cellulase transcripts in CLas(+) lemon and sweet orange leaf samples.[51,52] The increase in glucosidase/glucanase and cellulase expression in CLas(+) plants may correspond to the increased glucose concentration at 26 and 46 wpg (Figure 4), which could lead to the feedback inhibition of photosynthesis described above.[59] Cell wall fortification is often associated with plant defense as it strengthens the physical barrier between the host and the stressor.[60,61] Yet, we observed higher levels of both cell wall degrading and cell wall strengthening gene expression and protein abundance levels in infected plants at the same time (Figure 2), highlighting the crucial and complex role of cell wall regulation during CLas infection.

CLas Infection and the Stress Response in Citrus

Induction of the stress response was observed as early as 8 wpg (Figure 2). Notably, Kunitz family trypsin and protease inhibitor proteins were more abundant in infected plants at 8, 26, and 46 wpg and also had higher gene expression levels at 46 wpg (Figure S3 and Table S1). However, at 18 wpg, Kunitz proteins and a transcript were less abundant in CLas(+) plants. It was previously shown that rough lemon infected with CLas exhibited downregulation of a Kunitz family protein at 5 wpg but upregulation at 27 wpg.[52]

Miraculin-like proteins have sequence similarity with soybean Kunitz family trypsin inhibitor and have trypsin inhibitor activity.[44,45] Previous proteomic analysis revealed that miraculin-like proteins are downregulated in leaves from symptomatic CLas(+) lemon plants.[50] In another study, four miraculin-like proteins were shown to be higher in abundance in CLas-infected sweet orange plants before symptom development, and once the plant displayed HLB symptoms, the transcript for one miraculin-like protein was significantly higher.[26] Protease inhibitors have been shown to be induced following insect and pathogen attack.[76,77] Pathogens may secrete proteases to modify plant defense proteins and therefore overcome plant defense,[78] although both proteases and protease inhibitors are used by plants as well. Indeed, two miraculin-like proteins with trypsin inhibitor activity have been identified in Citrus jambhiri Lush and likely play a role in pathogen defense.[45] CLas has genes to encode an "offensive" type I secretion system, which would allow for extracellular secretion of degradative enzymes such as proteases.[79] Therefore, the increase in expression and abundance of trypsin and protease inhibitors might defend against CLas-secreted proteases and may prove an effective mechanism of CLas resistance.

Additionally, protease inhibitors may play a role in CLas acquisition and transmission by the psyllid vector. A recent study showed that aphids (Myzus persicae) fed a cysteine protease inhibitor had restored transmission of Potato leafroll virus.[80] Similarly, mosquitoes (Aedes aegypti) with lower trypsin gene expression and enzyme activity had higher rates of dengue virus infection.[81] Further investigation of the role of protease inhibitors in CLas-infected citrus may provide more information about the relationship between the pathogen, host, and vector.

CLas Alters the Navel Metabolome

Analysis of the citrus metabolome over the course of infection revealed several trends. First, we observed that some metabolites changed with infection in a consistent manner, such as asparagine and aspartate, which were generally lower in infected plants until 26 wpg (Figure 4). Many other metabolites, including sugars, several amino acids, and nucleosides, had higher median concentrations in infected plants between 8 wpg and 12 wpg but lower thereafter (Figure 4 and Table S5). The increase in concentration of several metabolites suggests the induction of plant defense. For example, proline, which has been shown to accumulate in response to a variety of abiotic and biotic stressors,[82,83] had a higher median concentration in infected plants compared to controls at every time point except 18 wpg. Arginine, which is a precursor for nitric oxide, had a higher median concentration in infected plants at most time points; at 26 and 46 wpg, the median concentrations were drastically higher in infected plants.[84]

Defense is costly and requires amino acids, sugars, and other small molecules as resources.[85,86] Defense gene expression and protein levels were generally higher in infected plants than controls at 8 wpg, but fewer defense genes and proteins were differentially expressed at 18 wpg (the overall number of differentially expressed genes and proteins was lower at 18 wpg than the other time points (Tables S1 and S4)). At 18 wpg, many metabolites were lower in concentration in CLas(+) plants relative to controls, which may coordinate with the low number of differentially expressed genes and differentially abundant proteins. Similar findings have been reported for microarray data of both lemons and oranges before FDR correction.[52] Whether this is direct inhibition of defense pathways by the bacterium or whether the absence of defense induction is a byproduct of pathogen evasion of host recognition requires further investigation.

■ CONCLUSIONS

CLas infection undoubtedly results in major changes to host metabolism. The results presented here represent greenhouse trees that were graft-inoculated with the Hacienda Heights, California, isolate of CLas and therefore may differ from mature field trees. Indeed, differences in development stages can affect resource pools and influence the plant response to stressors.[87−89] One key limitation of this study is the small number of replicates, which affected the power of the metabolomic analysis as the biological variability was high within (i.e., over time) and between plants. Nonetheless, we

provide broad and clear evidence that supports reports of changes of metabolism throughout infection from the transcript, protein, and metabolite perspectives. These changes are dynamic, with concerted changes in multiple systems, providing evidence of metabolism changes even during early infection. These findings may support future studies by informing of novel molecular targets for treatment and biomarkers for early detection of infection.

■ ASSOCIATED CONTENT

ⓢ Supporting Information

The Supporting Information is available free of charge at https://pubs.org/doi/10.1021/acs.jproteome.9b00616.

Figure S1, differentially expressed genes and metabolites involved in the phenylpropanoid pathway at 8, 18, 26, and 46 weeks post-grafting; Figure S2, differentially expressed genes and proteins involved in photosynthesis at 8, 18, 26, and 46 weeks post-grafting; and Figure S3, differentially expressed genes and proteins and all metabolites involved in the pathogen/pest stress response at 8, 18, 26, and 46 weeks post-grafting (PDF)

Table S1, normalized read counts of differentially expressed genes at 8, 18, 26, and 46 weeks post-grafting (XLSX)

Table S2, table of all significantly over/under-represented GO terms at 8, 18, 26, and 46 wpg from Blast2GO (XLSX)

Table S3, weighted protein spectral counts for all proteins identified at 8, 18, 26, and 46 wpg (XLSX)

Table S4, weighted protein spectral count table and GO term for each differentially abundant protein from Blast2GO (XLSX)

Table S5, median, minimum, and maximum metabolite concentrations for all time points (nmol/g dry material) (XLSX)

■ AUTHOR INFORMATION

Corresponding Author

Carolyn M. Slupsky − *University of California, Davis, Davis, California;* ⓞ orcid.org/0000-0002-5100-1594; Email: cslupsky@ucdavis.edu

Other Authors

Elizabeth L. Chin − *University of California, Davis, Davis, California*

John S. Ramsey − *USDA Agricultural Research Service, Ithaca, New York, and Boyce Thompson Institute for Plant Research, Ithaca, New York;* ⓞ orcid.org/0000-0003-1439-500X

Darya O. Mishchuk − *University of California, Davis, Davis, California*

Surya Saha − *Boyce Thompson Institute for Plant Research, Ithaca, New York*

Elizabeth Foster − *University of California, Davis, Davis, California*

Juan D. Chavez − *University of Washington, Seattle, Washington*

Kevin Howe − *USDA Agricultural Research Service, Ithaca, New York, and Boyce Thompson Institute for Plant Research, Ithaca, New York*

Xuefei Zhong − *University of Washington, Seattle, Washington*

MaryLou Polek − *National Clonal Germplasm Repository for Citrus & Dates, Riverside, California*

Kris E. Godfrey − *University of California, Davis, Davis, California*

Lukas A. Mueller − *Boyce Thompson Institute for Plant Research, Ithaca, New York*

James E. Bruce − *University of Washington, Seattle, Washington;* ⓞ orcid.org/0000-0001-6441-6089

Michelle Heck − *USDA Agricultural Research Service, Ithaca, New York, Boyce Thompson Institute for Plant Research, Ithaca, New York, and Cornell University, Ithaca, New York*

Complete contact information is available at: https://pubs.org/10.1021/acs.jproteome.9b00616

Notes

The authors declare no competing financial interest.

■ ACKNOWLEDGMENTS

■ ABBREVIATIONS

CLas, *Candidatus* Liberibacter asiaticus; HLB, Huanglongbing; qPCR, quantitative polymerase chain reaction; wpg, weeks post-grafting; GO, gene ontology; 4CL, 4-coumarate-CoA ligase; CCR, cinnamoyl-CoA reductase; CAD, cinnamyl alcohol dehydrogenase; PMEI, pectin methylesterase inhibitor; CCoAOMT, caffeoyl-CoA *O*-methyltransferase; COMT, caffeic acid *O*-methyltransferase; PSI, photosystem I; PSII, photosystem II; PLS-DA, partial least-squares-discriminant analysis; VIP, variable importance on the projection; PAL, phenylalanine ammonia lyase

■ REFERENCES

(1) Gottwald, T. R. Current epidemiological understanding of citrus Huanglongbing. *Annu. Rev. Phytopathol.* **2010**, *48*, 119−139.

(2) Bové, J. M. Huanglongbing: a destructive, newly-emerging, century-old disease of citrus. *Journal of Plant Pathology*; Springer: 2006, *88* (1), 7−37.

(3) Gottwald, T. R.; da Graça, J. V.; Bassanezi, R. B. Citrus Huanglongbing: the pathogen and its impact. In *Plant Health Progress*; APS Publications: 2007, 31.

(4) Grafton-Cardwell, E. E.; Stelinski, L. L.; Stansly, P. A. Biology and management of Asian citrus psyllid, vector of the Huanglongbing pathogens. *Annu. Rev. Entomol.* **2013**, *58*, 413−432.

(5) Grafton-Cardwell, E. E.; Godfrey, K. E.; Rogers, M. E.; Childers, C. C.; Stansly, P. A. *Asian citrus psyllid*; https://escholarship.org/uc/item/8vr1376d (Accessed 18 January 2016).

(6) Alvarez, S.; Rohrig, E.; Solís, D.; Thomas, M. H. Citrus greening disease (Huanglongbing) in Florida: economic impact, management and the potential for biological control. *Agric. Res.* **2016**, *5*, 109−118.

(7) Dala-Paula, B. M.; Plotto, A.; Bai, J.; Manthey, J. A.; Baldwin, E. A.; Ferrarezi, R. S.; Gloria, M. B. A. Effect of Huanglongbing or greening disease on orange juice quality, a review. *Front. Plant Sci.* **2019**, *9*, 1976.

(8) *California Department of Food and Agriculture. Citrus disease Huanglongbing detected in Hacienda Heights area of Los Angeles county.* https://www.cdfa.ca.gov/egov/Press_Releases/Press_Release.asp?PRnum=12-012 (Accessed 04 May 2017).

(9) *California Department of Food and Agriculture. Citrus disease Huanglongbing detected in San Gabriel area of Los Angeles county.* https://www.cdfa.ca.gov/egov/Press_Releases/Press_Release.asp?PRnum=15-031 (Accessed 06 January 2016).

(10) *Citrus Pest & Disease Prevention Program. California detections of citrus Huanglongbing up 160 Percent in 2018.* https://californiacitrusthreat.org/wp-content/themes/citrus/files/pdf/2018HLBRelease.CPDPP.PressRelease.2019.01.07.pdf (Accessed 15 September 2019).

(11) Bayles, B. R.; Thomas, S. M.; Simmons, G. S.; Grafton-Cardwell, E. E.; Daugherty, M. P. Spatiotemporal dynamics of the Southern California Asian citrus psyllid (Diaphorina citri) invasion. *PLoS One* **2017**, *12*, No. e0173226.

(12) *California Department of Food and Agriculture. Asian citrus psyllid detected in Sacramento.* https://www.cdfa.ca.gov/egov/Press_Releases/Press_Release.asp?PRnum=19-016 (Accessed 15 September 2019).

(13) *California Department of Food and Agriculture. Asian citrus psyllid detected in San Francisco.* https://www.cdfa.ca.gov/egov/Press_Releases/Press_Release.asp?PRnum=19-005 (Accessed 15 September 2019).

(14) Ha, P. T.; He, R.; Killiny, N.; Brown, J. K.; Omsland, A.; Gang, D. R.; Beyenal, H. Host-free biofilm culture of "*Candidatus* Liberibacter asiaticus," the bacterium associated with Huanglongbing. *Biofilm* **2019**, *1*, 100005.

(15) Fukushima, A.; Kusano, M.; Redestig, H.; Arita, M.; Saito, K. Integrated omics approaches in plant systems biology. *Curr. Opin. Chem. Biol.* **2009**, *13*, 532−538.

(16) Edwards, D.; Batley, J. Plant bioinformatics: from genome to phenome. *Trends Biotechnol.* **2004**, *22*, 232−237.

(17) Cho, K.; Shibato, J.; Agrawal, G. K.; Jung, Y.-H.; Kubo, A.; Jwa, N.-S.; Tamogami, S.; Satoh, K.; Kikuchi, S.; Higashi, T.; Kimura, S.; Saji, H.; Tanaka, Y.; Iwahashi, H.; Masuo, Y.; Rakwal, R. Integrated transcriptomics, proteomics, and metabolomics analyses to survey ozone responses in the leaves of rice seedling. *J. Proteome Res.* **2008**, *7*, 2980−2998.

(18) Casati, P.; Campi, M.; Morrow, D. J.; Fernandes, J. F.; Walbot, V. Transcriptomic, proteomic and metabolomic analysis of UV-B signaling in maize. *BMC Genomics* **2011**, *12*, 321.

(19) Amiour, N.; Imbaud, S.; Clément, G.; Agier, N.; Zivy, M.; Valot, B.; Balliau, T.; Armengaud, P.; Quilleré, I.; Cañas, R.; Tercet-Laforgue, T.; Hirel, B. The use of metabolomics integrated with transcriptomic and proteomic studies for identifying key steps involved in the control of nitrogen metabolism in crops such as maize. *J. Exp. Bot.* **2012**, *63*, 5017−5033.

(20) Barros, E.; Lezar, S.; Anttonen, M. J.; Van Dijk, J. P.; Röhlig, R. M.; Kok, E. J.; Engel, K. H. Comparison of two GM maize varieties with a near-isogenic non-GM variety using transcriptomics, proteomics and metabolomics. *Plant Biotechnol. J.* **2010**, *8*, 436−451.

(21) Slisz, A. M.; Breksa, A. P., III; Mishchuk, D. O.; McCollum, G.; Slupsky, C. M. Metabolomic analysis of citrus infection by 'Candidatus Liberibacter' reveals insight into pathogenicity. *J. Proteome Res.* **2012**, *11*, 4223−4230.

(22) Hung, W.-L.; Wang, Y. Metabolite profiling of *Candidatus* Liberibacter infection in Hamlin sweet oranges. *J. Agric. Food Chem.* **2018**, *66*, 3983−3991.

(23) Chin, E. L.; Mishchuk, D. O.; Breksa, A. P.; Slupsky, C. M. Metabolite signature of *Candidatus* Liberibacter asiaticus infection in two citrus varieties. *J. Agric. Food Chem.* **2014**, 6585.

(24) Martinelli, F.; Reagan, R. L.; Uratsu, S. L.; Phu, M. L.; Albrecht, U.; Zhao, W.; Davis, C. E.; Bowman, K. D.; Dandekar, A. M. Gene regulatory networks elucidating Huanglongbing disease mechanisms. *PLoS One* **2013**, *8*, No. e74256.

(25) Martinelli, F.; Uratsu, S. L.; Albrecht, U.; Reagan, R. L.; Phu, M. L.; Britton, M.; Buffalo, V.; Fass, J.; Leicht, E.; Zhao, W.; Lin, D.; D'Souza, R.; Davis, C. E.; Bowman, K. D.; Dandekar, A. M. Transcriptome profiling of citrus fruit response to Huanglongbing disease. *PLoS One* **2012**, *7*, No. e38039.

(26) Fan, J.; Chen, C.; Yu, Q.; Brlansky, R. H.; Li, Z.-G.; Gmitter, F. G., Jr. Comparative iTRAQ proteome and transcriptome analyses of sweet orange infected by "*Candidatus* Liberibacter asiaticus". *Physiol. Plant.* **2011**, *143*, 235−245.

(27) Zhong, Y.; Cheng, C.-z.; Jiang, N.-h.; Jiang, B.; Zhang, Y.-y.; Wu, B.; Hu, M.-l.; Zeng, J.-w.; Yan, H.-x.; Yi, G.-j.; Zhong, G.-y. Comparative transcriptome and iTRAQ proteome analyses of citrus root responses to Candidatus Liberibacter asiaticus infection. *PLoS One* **2015**, *10*, No. e0126973.

(28) Vidalakis, G. *Update on the Citrus Clonal Protection Program October 2008−September 2013.* http://citrusresearch.org/wp-content/uploads/Winter2014.pdf (Accessed 20 February 2015),

(29) Vidalakis, G.; Gumpf, D.; Polek, M.; Bash, J. The California Citrus Clonal Protection Program. In *Citrus Production Manual*; UC ANR: 2014; pp 117−130. University of California, Agriculture and Natural Resources: 2014.

(30) Li, W.; Hartung, J. S.; Levy, L. Quantitative real-time PCR for detection and identification of *Candidatus* Liberibacter species associated with citrus Huanglongbing. *J. Microbiol. Methods* **2006**, *66*, 104−115.

(31) Bolger, A. M.; Lohse, M.; Usadel, B. Trimmomatic: a flexible trimmer for Illumina sequence data. *Bioinformatics* **2014**, *30*, 2114−2120.

(32) Kim, D.; Pertea, G.; Trapnell, C.; Pimentel, H.; Kelley, R.; Salzberg, S. L. TopHat2: accurate alignment of transcriptomes in the presence of insertions, deletions and gene fusions. *Genome Biol.* **2013**, *14*, R36.

(33) Liao, Y.; Smyth, G. K.; Shi, W. featureCounts: an efficient general purpose program for assigning sequence reads to genomic features. *Bioinformatics* **2014**, *30*, 923−930.

(34) McCarthy, D. J.; Chen, Y.; Smyth, G. K. Differential expression analysis of multifactor RNA-Seq experiments with respect to biological variation. *Nucleic Acids Res.* **2012**, *40*, 4288−4297.

(35) Robinson, M. D.; McCarthy, D. J.; Smyth, G. K. edgeR: a Bioconductor package for differential expression analysis of digital gene expression data. *Bioinformatics* **2010**, *26*, 139−140.

(36) Conesa, A.; Götz, S. Blast2GO: A comprehensive suite for functional analysis in plant genomics. *Int. J. Plant Genomics* **2008**, *2008*, 619832.

(37) Lohse, M.; Nagel, A.; Herter, T.; May, P.; Schroda, M.; Zrenner, R.; Tohge, T.; Fernie, A. R.; Stitt, M.; Usadel, B. Mercator: a fast and simple web server for genome scale functional annotation of plant sequence data. *Plant Cell Environ.* **2014**, *37*, 1250−1258.

(38) Keller, A.; Nesvizhskii, A. I.; Kolker, E.; Aebersold, R. Empirical statistical model to estimate the accuracy of peptide identifications made by MS/MS and database search. *Anal. Chem.* **2002**, *74*, 5383−5392.

(39) Nesvizhskii, A. I.; Keller, A.; Kolker, E.; Aebersold, R. A statistical model for identifying proteins by tandem mass spectrometry. *Anal. Chem.* **2003**, *75*, 4646−4658.

(40) Vizcaíno, J. A.; Deutsch, E. W.; Wang, R.; Csordas, A.; Reisinger, F.; Ríos, D.; Dianes, J. A.; Sun, Z.; Farrah, T.; Bandeira, N.; Binz, P.-A.; Xenarios, I.; Eisenacher, M.; Mayer, G.; Gatto, L.; Campos, A.; Chalkley, R. J.; Kraus, H.-J.; Albar, J. P.; Martinez-

Bartolomé, S.; Apweiler, R.; Omenn, G. S.; Martens, L.; Jones, A. R.; Hermjakob, H. ProteomeXchange provides globally coordinated proteomics data submission and dissemination. *Nat. Biotechnol.* **2014**, *32*, 223−226.

(41) Vizcaíno, J. A.; Côté, R. G.; Csordas, A.; Dianes, J. A.; Fabregat, A.; Foster, J. M.; Griss, J.; Alpi, E.; Birim, M.; Contell, J. The PRoteomics IDEntifications (PRIDE) database and associated tools: status in 2013. *Nucleic Acids Res.* **2013**, *41*, D1063−D1069.

(42) Chin, E.; Godfrey, K.; Polek, M.; Slupsky, C. ¹H NMR analysis of *Citrus macrophylla* subjected to Asian citrus psyllid (*Diaphorina citri* Kuwayama) feeding. *Arthropod-Plant Interact.* **2017**, *11*, 901−909.

(43) Goodpaster, A. M.; Kennedy, M. A. Quantification and statistical significance analysis of group separation in NMR-based metabonomics studies. *Chemom. Intell. Lab. Syst.* **2011**, *109*, 162−170.

(44) Selvakumar, P.; Gahloth, D.; Tomar, P. P. S.; Sharma, N.; Sharma, A. K. Molecular evolution of miraculin-like proteins in soybean kunitz super-family. *J. Mol. Evol.* **2011**, *73*, 369−379.

(45) Tsukuda, S.; Gomi, K.; Yamamoto, H.; Akimitsu, K. Characterization of cDNAs encoding two distinct miraculin-like proteins and stress-related modulation of the corresponding mRNAs in *Citrus jambhiri* Lush. *Plant Mol. Biol.* **2006**, *60*, 125−136.

(46) Fell, D. A. Enzymes, metabolites and fluxes. *J. Exp. Bot.* **2004**, *56*, 267−272.

(47) Fernie, A. R.; Stitt, M. On the discordance of metabolomics with proteomics and transcriptomics: coping with increasing complexity in logic, chemistry, and network interactions scientific correspondence. *Plant Physiol.* **2012**, *158*, 1139−1145.

(48) Morgenthal, K.; Weckwerth, W.; Steuer, R. Metabolomic networks in plants: Transitions from pattern recognition to biological interpretation. *Biosystems* **2006**, *83*, 108−117.

(49) Nwugo, C. C.; Duan, Y.; Lin, H. Study on citrus response to Huanglongbing highlights a down-regulation of defense-related proteins in lemon plants upon 'Ca. Liberibacter asiaticus' infection. *PLoS One* **2013**, *8*, No. e67442.

(50) Nwugo, C. C.; Lin, H.; Duan, Y.; Civerolo, E. L. The effect of 'Candidatus Liberibacter asiaticus' infection on the proteomic profiles and nutritional status of pre-symptomatic and symptomatic grapefruit (*Citrus paradisi*) plants. *BMC Plant Biol.* **2013**, *13*, 59.

(51) Albrecht, U.; Bowman, K. D. Gene expression in *Citrus sinensis* (L.) Osbeck following infection with the bacterial pathogen *Candidatus* Liberibacter asiaticus causing Huanglongbing in Florida. *Plant Sci.* **2008**, *175*, 291−306.

(52) Fan, J.; Chen, C.; Yu, Q.; Khalaf, A.; Achor, D. S.; Brlansky, R. H.; Moore, G. A.; Li, Z.-G.; Gmitter, F. G., Jr. Comparative transcriptional and anatomical analyses of tolerant rough lemon and susceptible sweet orange in response to 'Candidatus Liberibacter asiaticus' infection. *Mol. Plant-Microbe Interact.* **2012**, *25*, 1396−1407.

(53) Berger, S.; Sinha, A. K.; Roitsch, T. Plant physiology meets phytopathology: plant primary metabolism and plant−pathogen interactions. *J. Exp. Bot.* **2007**, *58*, 4019−4026.

(54) Bilgin, D. D.; Zavala, J. A.; Zhu, J.; Clough, S. J.; Ort, D. R.; DeLucia, E. H. Biotic stress globally downregulates photosynthesis genes. *Plant Cell Environ.* **2010**, *33*, 1597−1613.

(55) Fan, J.; Chen, C.; Brlansky, R. H.; Gmitter, F. G., Jr.; Li, Z.-G. Changes in carbohydrate metabolism in *Citrus sinensis* infected with 'Candidatus Liberibacter asiaticus'. *Plant Pathol.* **2010**, *59*, 1037−1043.

(56) Freitas, D. D. S.; Carlos, E. F.; Gil, M. C. S. D. S.; Vieira, L. G. E.; Alcantara, G. B. NMR-based metabolomic analysis of Huanglongbing-asymptomatic and -symptomatic citrus trees. *J. Agric. Food Chem.* **2015**, *63*, 7582−7588.

(57) Hawkins, S. A.; Park, B.; Poole, G. H.; Gottwald, T.; Windham, W. R.; Lawrence, K. C. Detection of citrus Huanglongbing by Fourier transform infrared−attenuated total reflection spectroscopy. *Appl. Spectrosc.* **2010**, *64*, 100−103.

(58) Whitaker, D. C.; Giurcanu, M. C.; Young, L. J.; Gonzalez, P.; Etxeberria, E.; Roberts, P.; Hendricks, K.; Roman, F. Starch content of citrus leaves permits diagnosis of Huanglongbing in the warm season but not cool season. *Hortscience* **2014**, *49*, 757−762.

(59) Paul, M. J.; Pellny, T. K. Carbon metabolite feedback regulation of leaf photosynthesis and development. *J. Exp. Bot.* **2003**, *54*, 539−547.

(60) Malinovsky, F. G.; Fangel, J. U.; Willats, W. G. T. The role of the cell wall in plant immunity. *Front. Plant Sci.* **2014**, *5*, 178.

(61) Voigt, C. A. Callose-mediated resistance to pathogenic intruders in plant defense-related papillae. *Front. Plant Sci.* **2014**, *5*, 168.

(62) Rawat, N.; Kiran, S. P.; Du, D.; Gmitter, F. G.; Deng, Z. Comprehensive meta-analysis, co-expression, and miRNA nested network analysis identifies gene candidates in citrus against Huanglongbing disease. *BMC Plant Biol.* **2015**, *15*, 184.

(63) Fu, S.; Shao, J.; Zhou, C.; Hartung, J. S. Transcriptome analysis of sweet orange trees infected with 'Candidatus Liberibacter asiaticus' and two strains of Citrus Tristeza Virus. *BMC Genomics* **2016**, *17*, 349.

(64) Wang, Y.; Zhou, L.; Yu, X.; Stover, E.; Luo, F.; Duan, Y. Transcriptome profiling of Huanglongbing (HLB) tolerant and susceptible citrus plants reveals the role of basal resistance in HLB tolerance. *Front. Plant Sci.* **2016**, *7*, 933.

(65) Vanholme, R.; Demedts, B.; Morreel, K.; Ralph, J.; Boerjan, W. Lignin biosynthesis and structure. *Plant Physiol.* **2010**, *153*, 895−905.

(66) Boerjan, W.; Ralph, J.; Baucher, M. Ligninbiosynthesis. *Annu. Rev. Plant Biol.* **2003**, *54*, 519−546.

(67) Anterola, A. M.; Jeon, J.-H.; Davin, L. B.; Lewis, N. G. Transcriptional control of monolignol biosynthesis in *Pinus taeda*: Factors affecting monolignol ratios and carbon allocation in phenylpropanoid metabolism. *J. Biol. Chem.* **2002**, *277*, 18272−18280.

(68) Ralph, J.; Lapierre, C.; Marita, J. M.; Kim, H.; Lu, F.; Hatfield, R. D.; Ralph, S.; Chapple, C.; Franke, R.; Hemm, M. R.; van Doorsselaere, J.; Sederoff, R. R.; O'Malley, D. M.; Scott, J. T.; MacKay, J. J.; Yahiaoui, N.; Boudet, A.-M.; Pean, M.; Pilate, G.; Jouanin, L.; Boerjan, W. Elucidation of new structures in lignins of CAD- and COMT-deficient plants by NMR. *Phytochemistry* **2001**, *57*, 993−1003.

(69) Lapierre, C.; Pilate, G.; Pollet, B.; Mila, I.; Leplé, J.-C.; Jouanin, L.; Kim, H.; Ralph, J. Signatures of cinnamyl alcohol dehydrogenase deficiency in poplar lignins. *Phytochemistry* **2004**, *65*, 313−321.

(70) Van Acker, R.; Déjardin, A.; Desmet, S.; Hoengenaert, L.; Vanholme, R.; Morreel, K.; Laurans, F.; Kim, H.; Santoro, N.; Foster, C.; Goeminne, G.; Légée, F.; Pilate, G.; Ralph, J.; Boerjan, W. Different metabolic routes for coniferaldehyde -and sinapaldehyde with cinnamyl alcohol dehydrogenase1 deficiency. *Plant Physiol.* **2017**, *175*, 1018−1039.

(71) Monavarfeshani, A.; Mirzaei, M.; Sarhadi, E.; Amirkhani, A.; Khayam Nekouei, M.; Haynes, P. A.; Mardi, M.; Salekdeh, G. H. Shotgun proteomic analysis of the Mexican lime tree infected with "CandidatusPhytoplasma aurantifolia". *J. Proteome Res.* **2013**, *12*, 785−795.

(72) Mardi, M.; Farsad, L. K.; Gharechahi, J.; Salekdeh, G. H. In-depth transcriptome sequencing of mexican lime trees infected with *Candidatus* Phytoplasma aurantifolia. *PLoS One* **2015**, *10*, No. e0130425.

(73) Marowa, P.; Ding, A.; Kong, Y. Expansins: roles in plant growth and potential applications in crop improvement. *Plant Cell Rep.* **2016**, *35*, 949−965.

(74) Boava, L. P.; Cristofani-Yaly, M.; Machado, M. A. Physiologic, anatomic, and gene expression changes in *Citrus sunki, Poncirus trifoliata*, and their hybrids after 'Candidatus Liberibacter asiaticus' infection. *Phytopathology* **2017**, *107*, 590−599.

(75) Beffa, R. S.; Hofer, R.-M.; Thomas, M.; Meins, F., Jr. Decreased Susceptibility to Viral Disease of *β*−1,3-Glucanase-Deficient Plants Generated by Antisense Transformation. *Plant Cell* **1996**, *8*, 1001−1011.

(76) Ryan, C. A. Protease inhibitors in plants: genes for improving defenses against insects and pathogens. *Annu. Rev. Phytopathol.* **1990**, *28*, 425−449.

(77) Kim, J.-Y.; Park, S.-C.; Hwang, I.; Cheong, H.; Nah, J.-W.; Hahm, K.-S.; Park, Y. Protease inhibitors from plants with antimicrobial activity. *Int. J. Mol. Sci.* **2009**, *10*, 2860−2872.

(78) Jashni, M. K.; Mehrabi, R.; Collemare, J.; Mesarich, C. H.; de Wit, P. J. The battle in the apoplast: Further insights into the roles of proteases and their inhibitors in plant−pathogen interactions. *Front. Plant Sci.* **2015**, *6*, 584.

(79) Duan, Y.; Zhou, L.; Hall, D. G.; Li, W.; Doddapaneni, H.; Lin, H.; Liu, L.; Vahling, C. M.; Gabriel, D. W.; Williams, K. P.; Dickerman, A.; Sun, Y.; Gottwald, T. Complete genome sequence of citrus Huanglongbing bacterium,'*Candidatus* Liberibacter asiaticus' obtained through metagenomics. *Mol. Plant-Microbe Interact.* **2009**, *22*, 1011−1020.

(80) Pinheiro, P. V.; Ghanim, M.; Alexander, M.; Rebelo, A. R.; Santos, R. S.; Orsburn, B. C.; Gray, S.; Cilia, M. Host plants indirectly influence plant virus transmission by altering gut cysteine protease activity of aphid vectors. *Mol. Cell. Proteomics* **2017**, *16*, S230−S243.

(81) Angleró-Rodríguez, Y. I.; Talyuli, O. A.; Blumberg, B. J.; Kang, S.; Demby, C.; Shields, A.; Carlson, J.; Jupatanakul, N.; Dimopoulos, G. An *Aedes aegypti*-associated fungus increases susceptibility to dengue virus by modulating gut trypsin activity. *eLife* **2017**, *6*, e28844.

(82) Qamar, A.; Mysore, K. S.; Senthil-Kumar, M. Role of proline and pyrroline-5-carboxylate metabolism in plant defense against invading pathogens. *Front. Plant Sci.* **2015**, *6*, 503.

(83) Szabados, L.; Savouré, A. Proline: a multifunctional amino acid. *Trends Plant Sci.* **2010**, *15*, 89−97.

(84) Winter, G.; Todd, C. D.; Trovato, M.; Forlani, G.; Funck, D. Physiological implications of arginine metabolism in plants. *Front. Plant Sci.* **2015**, *6*, 534.

(85) Wu, J.; Baldwin, I. T. New insights into plant responses to the attack from insect herbivores. *Annu. Rev. Genet.* **2010**, *44*, 1−24.

(86) Schultz, J. C.; Appel, H. M.; Ferrieri, A. P.; Arnold, T. M. Flexible resource allocation during plant defense responses. *Front. Plant Sci.* **2013**, *4*, 324.

(87) Barton, K. E.; Koricheva, J. The ontogeny of plant defense and herbivory: characterizing general patterns using meta-analysis. *Am. Nat.* **2010**, *175*, 481−493.

(88) Orians, C. M.; Thorn, A.; Gómez, S. Herbivore-induced resource sequestration in plants: why bother? *Oecologia* **2011**, *167*, 1−9.

(89) Barton, K. E.; Boege, K. Future directions in the ontogeny of plant defence: understanding the evolutionary causes and consequences. *Ecol. Lett.* **2017**, *20*, 403−411.